

Two-dimensional electronic spectroscopy in the ultraviolet by a birefringent delay line

ROCIO BORREGO-VARILLAS,¹ AURELIO ORIANA,¹ LUCIA GANZER,¹ ANTON TRIFONOV,² IVAN BUCHVAROV,^{3,4} CRISTIAN MANZONI,¹ AND GIULIO CERULLO^{1,*}

¹IFN-CNR, Dipartimento di Fisica, Politecnico di Milano, Piazza Leonardo da Vinci 32, I-20133 Milano, Italy

²IBPhotonics Ltd., 19A Plovdivsko Pole Street, 1756 Sofia, Bulgaria

³Physics Department, Sofia University "St. Kliment Ohridski", 5 James Bourchier Blvd., 1164 Sofia, Bulgaria

⁴ITMO University, 197101St.-Petersburg, Russia

*giulio.cerullo@polimi.it

Abstract: We introduce a 2D electronic spectroscopy setup in the UV spectral range in the partially collinear pump-probe geometry. The required interferometrically phase-locked few-optical-cycle UV pulse pair is generated by combining a passive birefringent interferometer in the visible and nonlinear phase transfer. This is achieved by sum-frequency generation between the phase-locked visible pulse pair and narrowband infrared pulses. We demonstrate a pair of 16-fs, 330-nm pulses whose delay is interferometrically stable with an accuracy better than $\lambda/450$. 2DUV maps of pyrene solution probed in the UV and visible spectral ranges are demonstrated.

©2016 Optical Society of America

OCIS codes: (320.7160) Ultrafast technology; (260.7120) Ultrafast phenomena; (120.3180) Interferometry; (140.3610) Lasers, ultraviolet.

References and links

1. R. M. Hochstrasser, "Two-dimensional spectroscopy at infrared and optical frequencies," *Proc. Natl. Acad. Sci. U.S.A.* **104**(36), 14190–14196 (2007).
2. S. Mukamel, "Multidimensional femtosecond correlation spectroscopies of electronic and vibrational excitations," *Annu. Rev. Phys. Chem.* **51**(1), 691–729 (2000).
3. M. L. Cowan, J. P. Ogilvie, and R. J. D. Miller, "Two-dimensional spectroscopy using diffractive optics based phase-locked photon echoes," *Chem. Phys. Lett.* **386**(1–3), 184–189 (2004).
4. T. Brixner, I. V. Stiopkin, and G. R. Fleming, "Tunable two-dimensional femtosecond spectroscopy," *Opt. Lett.* **29**(8), 884–886 (2004).
5. L. P. DeFlores, R. A. Nicodemus, and A. Tokmakoff, "Two-dimensional Fourier transform spectroscopy in the pump-probe geometry," *Opt. Lett.* **32**(20), 2966–2968 (2007).
6. E. M. Grumstrup, S. H. Shim, M. A. Montgomery, N. H. Damrauer, and M. T. Zanni, "Facile collection of two-dimensional electronic spectra using femtosecond pulse-shaping technology," *Opt. Express* **15**(25), 16681–16689 (2007).
7. J. Sperling, A. Nemeth, J. Hauer, D. Abramavicius, S. Mukamel, H. F. Kauffmann, and F. Milota, "Excitons and Disorder in Molecular Nanotubes: A 2D Electronic Spectroscopy Study and First Comparison to a Microscopic Model," *J. Phys. Chem. A* **114**(32), 8179–8189 (2010).
8. T. Brixner, J. Stenger, H. M. Vaswani, M. Cho, R. E. Blankenship, and G. R. Fleming, "Two-dimensional spectroscopy of electronic couplings in photosynthesis," *Nature* **434**(7033), 625–628 (2005).
9. G. S. Engel, T. R. Calhoun, E. L. Read, T.-K. Ahn, T. Mancal, Y.-C. Cheng, R. E. Blankenship, and G. R. Fleming, "Evidence for wavelike energy transfer through quantum coherence in photosynthetic systems," *Nature* **446**(7137), 782–786 (2007).
10. E. Collini, C. Y. Wong, K. E. Wilk, P. M. G. Curmi, P. Brumer, and G. D. Scholes, "Coherently wired light-harvesting in photosynthetic marine algae at ambient temperature," *Nature* **463**(7281), 644–647 (2010).
11. D. B. Turner and K. A. Nelson, "Coherent measurements of high-order electronic correlations in quantum wells," *Nature* **466**(7310), 1089–1092 (2010).
12. K. W. Stone, K. Gundogdu, D. B. Turner, X. Li, S. T. Cundiff, and K. A. Nelson, "Two-quantum 2D FT electronic spectroscopy of biexcitons in GaAs quantum wells," *Science* **324**(5931), 1169–1173 (2009).
13. J. Jiang and S. Mukamel, "Two-Dimensional Ultraviolet (2DUV) Spectroscopic Tools for Identifying Fibrillation Propensity of Protein Residue Sequences," *Angew. Chem. Int. Ed. Engl.* **49**(50), 9666–9669 (2010).

14. Q. Li, A. Giussani, J. Segarra-Martí, A. Nenov, I. Rivalta, A. A. Voityuk, S. Mukamel, D. Roca-Sanjuán, M. Garavelli, and L. Blancafort, "Multiple Decay Mechanisms and 2D-UV Spectroscopic Fingerprints of Singlet Excited Solvated Adenine-Uracil Monophosphate," *Chemistry* **22**(22), 7497–7507 (2016).
15. A. Nenov, I. Rivalta, G. Cerullo, S. Mukamel, and M. Garavelli, "Disentangling Peptide Configurations via Two-Dimensional Electronic Spectroscopy: Ab Initio Simulations Beyond the Frenkel Exciton Hamiltonian," *J. Phys. Chem. Lett.* **5**(4), 767–771 (2014).
16. B. A. West, J. M. Womick, and A. M. Moran, "Probing ultrafast dynamics in adenine with mid-UV four-wave mixing spectroscopies," *J. Phys. Chem. A* **115**(31), 8630–8637 (2011).
17. B. A. West and A. M. Moran, "Two-dimensional electronic spectroscopy in the ultraviolet wavelength range," *J. Phys. Chem. Lett.* **3**(18), 2575–2581 (2012).
18. U. Selig, C. F. Schleussner, M. Foerster, F. Langhojer, P. Nuernberger, and T. Brixner, "Coherent two-dimensional ultraviolet spectroscopy in fully noncollinear geometry," *Opt. Lett.* **35**(24), 4178–4180 (2010).
19. V. Prokhorenko, A. Picchiotti, S. Maneshi, and D. Miller, "Broadband Electronic Two-Dimensional Spectroscopy in the Deep UV," in 19th International Conference on Ultrafast Phenomena, OSA Technical Digest (online) (Optical Society of America, 2014), paper 09.Wed.A.4.
20. C. H. Tseng, S. Matsika, and T. C. Weinacht, "Two-dimensional ultrafast fourier transform spectroscopy in the deep ultraviolet," *Opt. Express* **17**(21), 18788–18793 (2009).
21. C. H. Tseng, P. Sándor, M. Kotur, T. C. Weinacht, and S. Matsika, "Two-dimensional fourier transform spectroscopy of adenine and uracil using shaped ultrafast laser pulses in the deep UV," *J. Phys. Chem. A* **116**(11), 2654–2661 (2012).
22. N. Krebs, I. Pugliesi, J. Hauer, and E. Riedle, "Two-dimensional Fourier transform spectroscopy in the ultraviolet with sub-20 fs pump pulses and 250 – 720 nm supercontinuum probe," *New J. Phys.* **15**(8), 085016 (2013).
23. G. Auböck, C. Consani, F. van Mourik, and M. Chergui, "Ultrabroadband femtosecond two-dimensional ultraviolet transient absorption," *Opt. Lett.* **37**(12), 2337–2339 (2012).
24. C. Consani, G. Auböck, F. van Mourik, and M. Chergui, "Ultrafast tryptophan-to-heme electron transfer in myoglobins revealed by UV 2D spectroscopy," *Science* **339**(6127), 1586–1589 (2013).
25. D. Brida, C. Manzoni, and G. Cerullo, "Phase-locked pulses for two-dimensional spectroscopy by a birefringent delay line," *Opt. Lett.* **37**(15), 3027–3029 (2012).
26. J. Réhault, M. Maiuri, A. Oriana, and G. Cerullo, "Two-dimensional electronic spectroscopy with birefringent wedges," *Rev. Sci. Instrum.* **85**(12), 123107 (2014).
27. R. B. Varillas, A. Candeo, D. Viola, M. Garavelli, S. De Silvestri, G. Cerullo, and C. Manzoni, "Microjoule-level, tunable sub-10 fs UV pulses by broadband sum-frequency generation," *Opt. Lett.* **39**(13), 3849–3852 (2014).
28. M. Zavelani-Rossi, G. Cerullo, S. De Silvestri, L. Gallmann, N. Matuschek, G. Steinmeyer, U. Keller, G. Angelow, V. Scheuer, and T. Tschudi, "Pulse compression over a 170-THz bandwidth in the visible by use of only chirped mirrors," *Opt. Lett.* **26**(15), 1155–1157 (2001).
29. P. Bowlan, P. Gabolde, A. Shreenath, K. McGresham, R. Trebino, and S. Akturk, "Crossed-beam spectral interferometry: a simple, high-spectral-resolution method for completely characterizing complex ultrashort pulses in real time," *Opt. Express* **14**(24), 11892–11900 (2006).
30. S. A. Akhmanov, V. A. Vysloukh, and A. S. Chirkin, *Optics of Femtosecond Laser Pulses* (American Institute of Physics, New York, 1992).
31. H. S. Tan, E. Schreiber, and W. S. Warren, "High-resolution indirect pulse shaping by parametric transfer," *Opt. Lett.* **27**(6), 439–441 (2002).
32. L. Lepetit, G. Chériaux, and M. Joffre, "Linear techniques of phase measurement by femtosecond spectral interferometry for applications in spectroscopy," *J. Opt. Soc. Am. B* **12**(12), 2467–2474 (1995).
33. S. Witte, V. T. Tenner, D. W. E. Noom, and K. S. E. Eikema, "Lensless diffractive imaging with ultra-broadband table-top sources: from infrared to extreme-ultraviolet wavelengths," *Light Sci. Appl.* **3**(3), e163 (2014).
34. S. Shimizu, Y. Nabekawa, M. Obara, and K. Midorikawa, "Spectral phase transfer for indirect phase control of sub-20-fs deep UV pulses," *Opt. Express* **13**(17), 6345–6353 (2005).
35. J. R. Birge, R. Ell, and F. X. Kärtner, "Two-dimensional spectral shearing interferometry for few-cycle pulse characterization," *Opt. Lett.* **31**(13), 2063–2065 (2006).
36. R. Borrego-Varillas, A. Oriana, F. Branchi, S. De Silvestri, G. Cerullo, and C. Manzoni, "Optimized ancillae generation for ultra-broadband two-dimensional spectral-shearing interferometry," *J. Opt. Soc. Am. B* **32**(9), 1851–1855 (2015).
37. P. A. Tekavec, K. L. M. Lewis, F. D. Fuller, J. A. Myers, and J. P. Ogilvie, "Toward Broad Bandwidth 2-D electronic Spectroscopy: Correction of Chirp From a Continuum Probe," *IEEE J.S.T.Q. E* **18**(1), 210–217 (2012).
38. M. Raytchev, E. Pandurski, I. Buchvarov, C. Modrakowski, and T. Fiebig, "Bichromophoric Interactions and Time-Dependent Excited State Mixing in Pyrene Derivatives. A Femtosecond Broad-Band Pump–Probe Study," *J. Phys. Chem. A* **107**(23), 4592–4600 (2003).

1. Introduction

Two-dimensional electronic spectroscopy (2DES) is the most advanced ultrafast optical spectroscopy technique available to date, allowing to measure the full third-order nonlinear optical response of the system under study [1]. 2DES is a form of Fourier transform (FT) spectroscopy, which achieves resolution in the excitation frequency by varying with interferometric precision the delay between two ultrashort excitation pulses and performing the FT of the delay-dependent nonlinear signal; in this way, it overcomes the limitations of standard transient absorption spectroscopy, providing simultaneously high temporal and spectral resolution [2]. By spreading the information content of the nonlinear signal on two frequency axes, the excitation and detection frequencies, 2DES allows to measure the homogeneous linewidths of optical transitions and to visualize couplings and energy transfer processes between different transitions.

Two experimental configurations have been demonstrated for 2DES: the heterodyne detected three-pulse photon echo (3PPE) [3,4] and the partially collinear pump-probe geometry [5,6]. The first scheme adopts a non-collinear four-wave mixing geometry and fully resolves in amplitude and phase the nonlinear signal, generated in the phase-matched direction, by spectral interferometry with a fourth heterodyning pulse, acting as local oscillator. In the second scheme, a pair of collinear pump pulses are non-collinearly combined with a time-delayed probe pulse, generating a nonlinear signal which is heterodyned by the probe pulse itself (self-heterodyning configuration). For both configurations, the technical challenge lies in the generation of phase-locked pulses, which are required in order to perform the FT of the nonlinear signal.

2DES has been successfully applied in the infrared and visible spectral ranges, targeting molecular aggregates [7], photosynthetic light harvesting complexes [8–10] and semiconductors [11,12]. Its extension to the UV range (2DUV spectroscopy) is extremely promising for the study of biomolecules such as DNA and proteins [13,14] and also because it enables to excite small molecules, which allow benchmarking experiments with high level photochemical computations [15]. There are however significant technical challenges associated with 2DUV spectroscopy: (i) due to the short wavelengths, the requirement of interferometric stability translates into a tighter control of the pump pulses delay; (ii) due to the closeness to electronic resonances, material propagation in the UV introduces a very high dispersion, so that it becomes very difficult to deliver few-optical-cycle transform-limited (TL) pulses to the experiment point.

So far a number of schemes for 2DUV spectroscopy have been proposed and experimentally demonstrated, both in the 3PPE and in the pump-probe geometry. Moran *et al.* employed the non-collinear boxcar geometry, using diffractive optics for the generation of phase-locked pairs of 20-fs, 260-nm pulses from a Ti:sapphire laser broadened in an hollow-core fiber, to study relaxation dynamics in adenine and thymine [16,17]. Selig *et al.* developed a fully non-collinear miniaturized all-reflective setup driven by 50-fs pulses produced by second-harmonic generation (SHG) of a non-collinear optical parametric amplifier (NOPA) [18]. A similar setup but with greatly increased spectral bandwidth, obtained by SHG of a visible NOPA with achromatic phase matching, was reported by Prokhorenko *et al.* [19]. Weinacht *et al.* developed a 2DUV setup in the partially collinear pump-probe geometry using an acousto-optic-modulator based pulse shaper for the generation of the phase-locked pump pulses [20]. Using 50-fs, 260-nm pulses obtained as the third harmonic of a Ti:sapphire laser system, they studied ultrafast relaxation processes in adenine and uracyl nucleobases [21]. A similar system was proposed by Riedle *et al.*, in which an acousto-optic programmable dispersive filter was used as pulse shaper, obtaining sub-16-fs phase-locked UV pulse pairs [22]. All these configurations generate the pump pairs by directly manipulating the UV pulses, which poses serious challenges in spectral phase control especially when dealing with ultrabroadband pulses. Finally, Chergui *et al.* demonstrated a simple and robust approach to 2DUV spectroscopy, in which a broadband and spectrally

resolved probe pulse is combined with a frequency tunable, narrowband pump pulse [23,24]. Since each of the proposed configurations has advantages but also drawbacks and limitations, there is an ongoing research in the development of experimental approaches to 2DUV spectroscopy.

Recently, we introduced a novel configuration for 2DES in the partially collinear pump-probe geometry, employing a passive birefringent interferometer for the generation of the phase-locked pump pulse pair [25,26]. The interferometer, called Translating-Wedge-based Identical pulse eNcoding System (TWINS), exploits birefringence to generate two phase-locked collinear pump pulses with very high delay precision. TWINS has the advantages of simplicity, compactness, low cost and broad acceptance bandwidth; however, its direct application to the UV range is challenging, because its refractive optical components introduce a large amount of dispersion which would be very difficult to compensate. To overcome this difficulty and generate phase-locked UV pulses, in this work we combine pulse shaping by TWINS in the visible with frequency up-conversion and nonlinear phase transfer. We generate ultrashort UV pulse pairs by sum-frequency generation (SFG) between a pair of phase-locked visible pulses and a quasi-monochromatic infrared (IR) beam. This approach allows us to avoid the very high dispersion introduced by direct pulse shaping in the UV, while fulfilling the phase stability requirements. We demonstrate 16-fs UV pulse pairs with a spectrum extending from 320 to 360 nm and relative delay controlled to an accuracy better than $\lambda/450$. The system is applied to proof-of-principle 2DUV spectroscopy experiments in the partially collinear pump-probe geometry.

2. Generation of phase-locked UV pulses

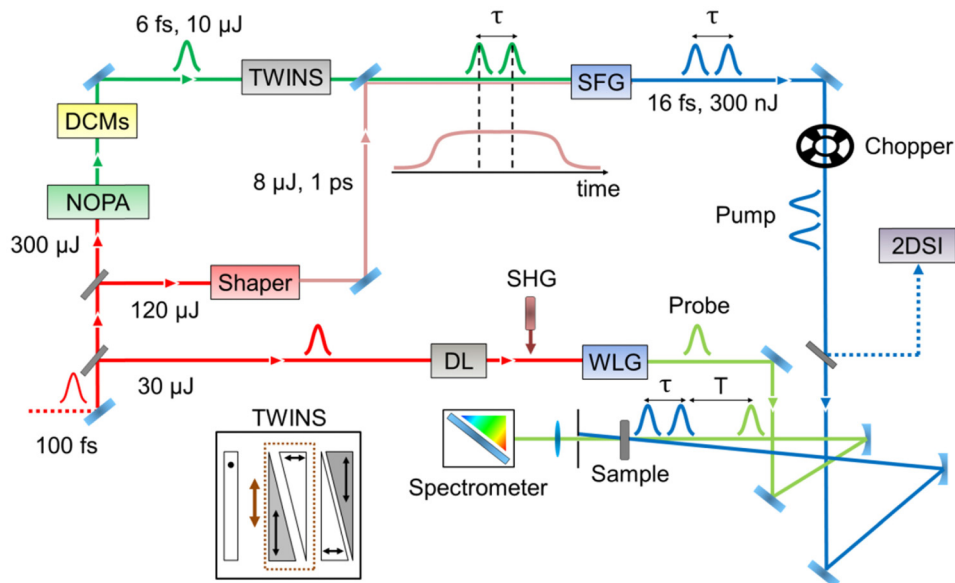


Fig. 1. Experimental 2DUV setup. DCMs: two pairs of double chirped mirrors used to compress the NOPA and pre-compensate for the TWINS dispersion, respectively; SFG: sum-frequency generation; DL: delay line; WLG: white-light generation.

Figure 1 shows the experimental setup used for phase-locked UV pulses generation and 2DUV spectroscopy. The system is driven by a 450- μ J fraction of the output of an amplified Ti:sapphire laser (Coherent Libra), producing 100-fs pulses at 1-kHz repetition rate and 800-nm wavelength. The beam is split in three lines, with energies of 300 μ J, 120 μ J and 30 μ J. These lines are used respectively to pump a visible NOPA, to generate narrowband IR pulses for frequency up-conversion and to generate a broadband white light continuum (WLC) used

as a probe. The first line drives a single-pass blue-pumped visible NOPA [27], which produces 10- μ J pulses, with a spectrum extending from 510 to 720 nm. The NOPA pulses, compressed to nearly TL 7-fs duration by multiple reflections onto pairs of dielectric double-chirped mirrors (DCMs) [28], are sent to a TWINS interferometer generating two variable-delay, collinear phase-locked replicas. The TWINS device follows the design reported in [26] and consists of a sequence of wedges of α -barium borate (α -BBO) providing a delay τ up to 500 fs. An additional pair of DCMs compensates for the dispersion introduced by the TWINS and retrieves nearly TL duration for the visible pulse pairs, as measured by the Spatial Encoded Arrangement for Temporal Analysis by Dispersing a Pair of Light E-fields (SEA-TADPOLE) technique [29].

The broadband phase-locked visible replicas produced by TWINS are subsequently up-converted to the UV range by SFG with a fraction of the 800-nm source, derived from the second line, using a β -barium borate (BBO) crystal in a broadband Type-II configuration ($\theta = 45.8^\circ$, crystal thickness 50 μ m). Considering the SFG process $\omega_1 + \omega_2 = \omega_3$, the Type-II configuration ($e_1 + o_2 \rightarrow e_3$) in BBO has a broad acceptance bandwidth for the ordinary axis and considerably narrower one for the extraordinary axis [27]; by polarizing the visible pulses along the ordinary direction and the narrowband field along the extraordinary one, it is possible to obtain efficient transfer of the broad visible bandwidth to the UV. To ensure uniform up-conversion at all delays of the visible pulse pair, the 800-nm beam is spectrally filtered by a 4- f zero dispersion pulse shaper, consisting of a reflection grating and a spherical mirror with an aperture in the Fourier plane, to obtain a narrowband \sim 1 ps pulse with 8- μ J energy. The overall energy of the up-converted pulse pair is 300 nJ.

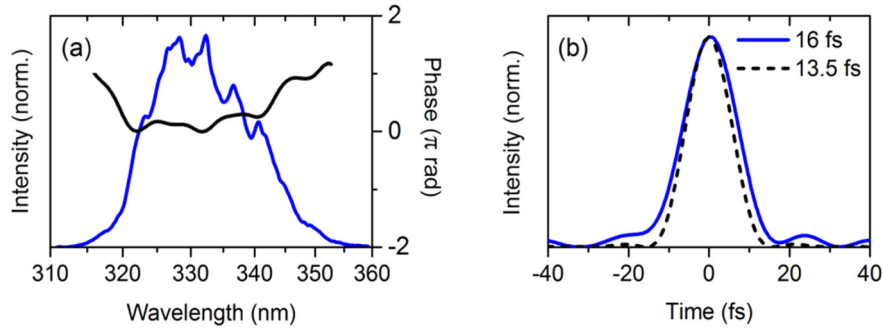


Fig. 2. (a) Spectral intensity (blue line) and phase (black line) and (b) temporal intensity profiles of each UV pulse replica. Dashed black line of panel (b) corresponds to a TL pulse.

To understand the process of SFG with a pulse pair, we consider up-conversion of a broadband visible pulse $\tilde{E}_2(\omega)$ by a narrowband gate pulse $\tilde{E}_1(\omega)$. The SFG pulse $\tilde{E}_3(\omega)$ can be written as [30, 31]:

$$\tilde{E}_3(\omega) \propto \int_{-\infty}^{+\infty} \tilde{E}_2(\omega') \tilde{E}_1(\omega - \omega') d\omega' \quad (1)$$

which, for the case of a nearly monochromatic gate, $\tilde{E}_1(\omega) \equiv \delta(\omega - \bar{\omega}_1)$ becomes: $\tilde{E}_3(\omega) \equiv \tilde{E}_2(\omega - \bar{\omega}_1)$ showing that the SFG pulse is a replica of the visible pulse blue-shifted by $\bar{\omega}_1$. SFG with a quasi-monochromatic pulse thus transfers to the UV with high fidelity also the spectral phase of the visible pulses, and ensures the generation of a pair of high-quality phase-locked UV pulses. The gate pulse $\tilde{E}_1(\omega)$ can be considered monochromatic when its bandwidth $\Delta\omega_1$ is much narrower than the width of any feature in the broadband spectrum $\tilde{E}_2(\omega)$. Since a pulse pair with relative delay τ presents spectral interference fringes with

period $\Delta\omega_2 = 2\pi/\tau$ [32], the monochromaticity condition becomes $\Delta\omega_1 \ll 2\pi/\tau$. Considering the typical dephasing times of UV transitions, the maximum delay values required for 2DUV spectroscopy are $\tau = 100$ -200 fs, so that the monochromaticity condition is satisfied very well in our case with ≈ 1 -ps IR pulses. Equation (1) also shows that direct SHG of the visible pulse pair would not allow the high fidelity transfer of their temporal structure to the UV. To avoid this problem Witte *et al.*, when producing phase-locked XUV pulse pairs by high harmonic generation of IR pulse pairs, had to use a non-collinear geometry [33].

Particular attention has been devoted to the compression of the UV pulses, controlling their spectral phase by the mechanism of indirect phase transfer, which shifts the spectral phase of the NOPA pulse to the up-converted light [31,34]. This allows the fine tuning of the UV spectral phase simply by acting on the chirp in the visible spectral range; by controlling the number of reflections on the DCM pairs as well as the fine insertion of one of the static TWINS wedges, we compensate for the positive chirp acquired by the UV pulses during propagation to the measurement point. The temporal characterization of each of the UV pulse replicas (Fig. 2(a)) was performed using a modified version of the two-dimensional spectral-shearing interferometry (2DSI) technique [35], which we recently introduced [36], revealing 16-fs pulses in the range 320-360 nm (Fig. 2(b)), very close to the 13.5-fs TL duration.

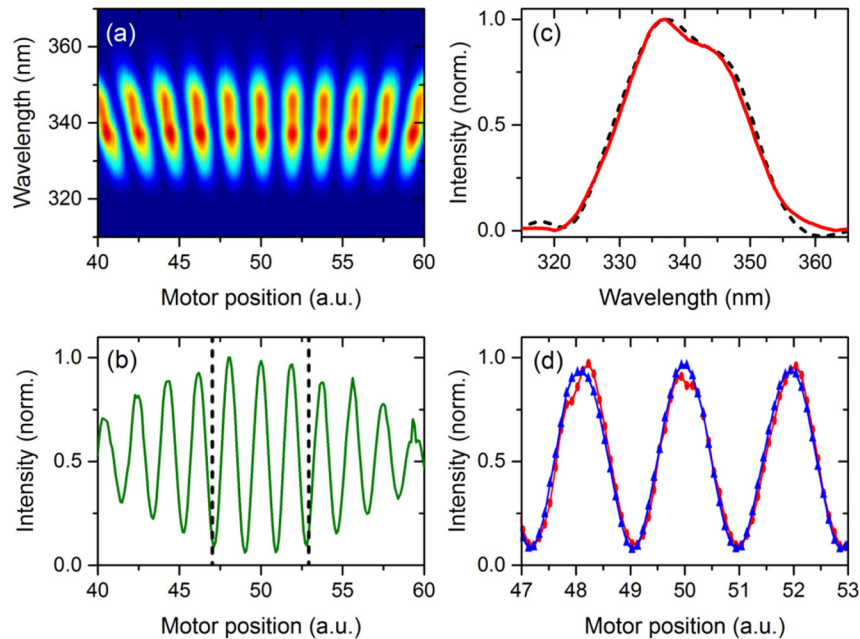


Fig. 3. (a) Spectrally-resolved linear autocorrelation of the UV pulses. (b) Autocorrelation trace obtained by integrating the 2D autocorrelation map along the wavelength axis. (c) Power spectra of the UV pulses. Black dashed line: measured spectrum obtained by integrating the 2D autocorrelation map along the motor position axis; red solid line: spectrum from the FT of the autocorrelation trace. (d) Blue and red: zoom (between the dashed vertical lines of panel (b)) of two correlation traces acquired at 30 minutes distance.

We first characterized the collinear UV pulse pair by spectral interferometry. Figure 3(a) shows a spectrally-resolved linear autocorrelation of the UV pulses, as a function of the insertion of the TWINS wedges, expressed by the unitless motor position. This measurement allows a characterization of the TWINS system: integration along the frequency axis gives the linear autocorrelation trace (panel (b)), which after Fourier transform and recalibration of the frequency axis provides the power spectrum of the pulses (red solid line, panel (c)). The excellent agreement with the measured power spectrum (black dashed line in panel (c))

confirms the accuracy of the technique. Note that to obtain the source spectrum by Fourier transforming the autocorrelation, it is first necessary to calibrate the device. This cannot be performed by simply rescaling the time axis (or the motor position) because the differential dispersion introduced by the birefringent wedges is frequency-dependent, and at a specific motor position, the delay accumulated by each spectral component depends on its frequency. For this reason, calibration is performed in the frequency domain, as described in [25, 26]: a horizontal cut of the map in Fig. 3(a) is the electric field correlation for the corresponding spectral component. Since the motor position is typically recorded in motor “steps”, by taking a Fourier transform one gets the pseudofrequency (in units of “1/steps”) of the oscillation. By associating the pseudofrequency of each spectral component to its optical frequency, we obtain the calibration of that component. Following this procedure for all the optical frequencies, gives the full calibration of the device. The same pseudofrequency-to-frequency calibration curve is also applied to produce the 2DUV map from the time traces, as detailed later.

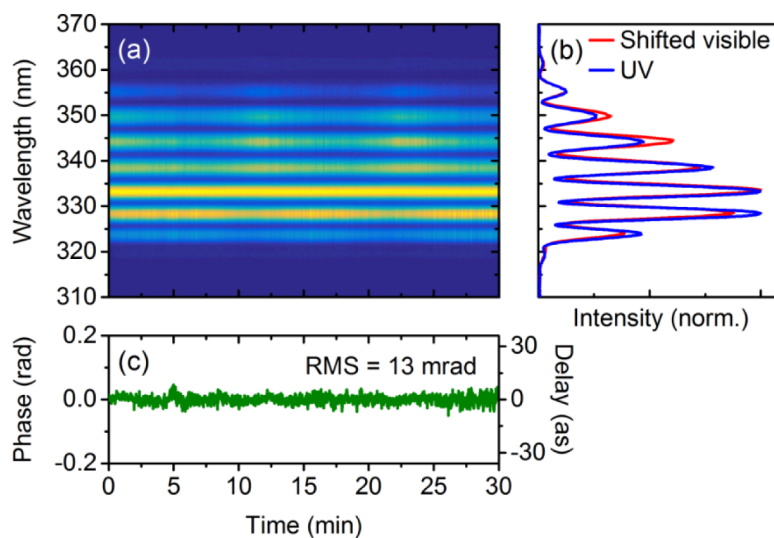


Fig. 4. (a) Sequence of UV spectral interference fringes acquired for 30 min at a fixed position of the wedges. (b) Interferogram of UV pulses (blue line, obtained as a cut of panel (a)) and of visible pulses from NOPA, blue-shifted by 375 THz (800 nm) (red line). (c) Phase fluctuations of the interferogram reported in (a). The delay fluctuation (right axis) is also reported for a carrier wavelength of 340 nm.

To test the long-term stability of our UV pulse pair generator, we acquired two linear autocorrelations at 30 minutes distance under the same experimental conditions: a portion of the frequency integrated autocorrelations is shown in Fig. 3(d). The very high reproducibility of the traces demonstrates the accuracy and reliability of our pulse pair generator. The TWINS system is intrinsically phase stable since the two pulse replicas propagate along a common path; to verify that this property holds also for the up-converted pulse pair, we recorded a sequence of interferograms for a fixed pulse delay (75 fs), as shown in Fig. 4(a). The spectra were acquired every second, with acquisition time of 4 ms (4 integrated pulses at 1 kHz repetition rate). The phase of the fringes, displayed in panel (c), fluctuates with RMS of ≈ 13 mrad (better than $\lambda/450$) over 30 minutes. Such fluctuations account for both the phase-stability of the pulse replicas and the sensitivity of the measurement. If we conservatively attribute all the fluctuations to the phase jitter, we get phase delay fluctuations of 2.3 attoseconds at 340-nm wavelength, showing that the SFG process does not alter the phase-locking of the pulse pair provided by TWINS. Interferometry also allows to compare the spectral phase of the visible NOPA pulses with that of the UV pulses: panel (b) displays the

interferogram of the UV pulses (blue line, obtained as a cut of the map in panel (a)) and the independently measured interferogram of the visible NOPA pulses (red line), translated to the UV spectral range by numerically blue-shifting the frequency axis by 375 THz (corresponding to the 800-nm gate). The excellent agreement between the two patterns confirms that we are in the regime of perfect nonlinear phase-transfer and that the gate pulse is sufficiently monochromatic. Taken together, these measurements show that our up-conversion scheme is able to produce phase-locked few-optical-cycle UV pulses to be employed in 2DUV spectroscopy.

3. Proof of principle of 2DUV spectroscopy

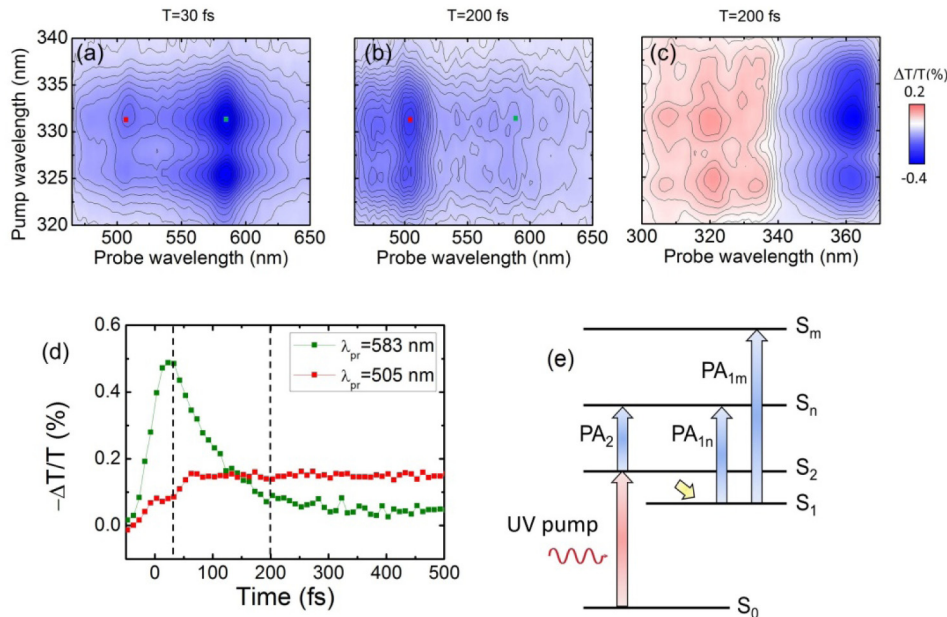


Fig. 5. 2DUV maps of pyrene probing in the visible (a-b) and the UV (c) range. (d) Dynamics at selected cross peaks showing the $S_2 \rightarrow S_1$ internal conversion process. (e) Sketch of the electronic transitions in pyrene probed in our experiments.

To test the 2DUV setup, we performed preliminary spectroscopy measurements employing the UV pulse pair as pump, and a WLC as probe. The WLC is generated by focusing either the fundamental or the second-harmonic of Ti:sapphire in a 3-mm CaF_2 plate, which allows us to probe in the spectral ranges 320-700 nm and 250-380 nm, respectively. The measurements were performed on pyrene ($\text{C}_{16}\text{H}_{10}$, Sigma Aldrich) dissolved in methanol (30 mM concentration). A 2DUV measurement is performed by fixing the pump-probe delay T and acquiring a set of differential transmission ($\Delta T/T$) spectra as a function of the delay τ between the pumps. Fourier transform of the delay-dependent nonlinear signal and application of the calibration curve provide a 2DUV map. In our measurement, the maximum delay between the pump pulses is 220 fs at 330 nm, which corresponds to spectral resolution of 1.66 nm along the pump axis.

Figure 5(a) and 5(b) report chirp-corrected 2DUV maps [37] recorded with our setup when probing in the visible spectral range (450-670 nm window). Our broadband UV pump pulse overlaps with the 0-0 $S_0 \rightarrow S_2$ transition and partially with its first vibronic replica, leading to the detection of two peaks along the pump wavelength axis. According to the energy level scheme of pyrene shown in Fig. 5(e), UV photoexcitation brings the pyrene to the bright excited state S_2 , from which it quickly decays to the S_1 state through internal conversion via a conical intersection [38]. At early pump-probe delays ($T = 30$ fs, Fig. 4(a))

we observe a strong negative cross peak at (332,580) nm, which is assigned the $S_2 \rightarrow S_n$ photo-induced absorption (PA); the quick decay of this peak at $T = 200$ fs (Fig. 5(b)) is associated with the build-up of a cross peak at (332,505) nm, assigned to the $S_1 \rightarrow S_n$ PA. The dynamics of these cross peaks, shown in Fig. 5(d), tracks the $S_2 \rightarrow S_1$ conical intersection occurring on the 100-fs timescale. Finally, Fig. 5(c) presents measurements with UV probe (300-380 nm window) at a delay $T = 200$ fs: the three positive peaks at 307 nm, 320 nm and 334 nm correspond to the photobleaching of the transitions from the ground state to the vibrational progression of the S_2 excited state, whereas the negative peak at 365 nm is due to the PA associated with the $S_1 \rightarrow S_m$ transition. These results are in good agreement with previous ultrafast studies on pyrene [22, 38].

4. Conclusions

In this work we have introduced a novel approach to 2DUV spectroscopy which combines the TWINS passive birefringent interferometer with parametric phase transfer. TWINS generates in a simple, compact and cost-effective way two phase-locked replicas of the few-optical-cycle pulses from a visible NOPA, which are then up-converted to the UV by SFG with a narrowband IR pulse. The up-conversion process shifts with high fidelity the spectral phase of the visible pulses to the UV, resulting in the generation of 16-fs pulse-pairs covering the 320-360 nm range, with relative delay controlled with a stability better than $\lambda/450$. The setup has been applied to preliminary 2DUV measurements probing the internal conversion process in pyrene. Our approach is quite general and can be extended to different spectral ranges for which dispersion compensation is not straightforward. In particular, it will be interesting to cover, by upconversion of the broadband NOPA with a narrowband visible OPA, the 250-300 nm wavelength region matching the $\pi \rightarrow \pi^*$ transitions of DNA nucleobases and aromatic aminoacids.

Funding

European Research Council: Advanced Grant STRATUS (ERC-2011-AdG No. 291198) and Proof of Concept Grant MISSION (ERC-2014-POC No. 665635). Marie Curie actions (FP7-PEOPLE-IEF-2012). Horizon 2020 (654148, Laserlab-Europe).

Acknowledgments

The authors would like to thank Julien Rehaut for his help with the 2D spectroscopy software.